# A Theoretical Analysis of Three-Dimensional Eye Position Measurement Using Polar Cross-Correlation

Thomas Haslwanter and Steven T. Moore

*Abstract*— **Polar cross-correlation is a commonly used technique for determination of torsional eye position from video images. At eccentric eye positions, the projection of the sampling window onto the image plane of the camera is translated and deformed due to the spherical shape of the eyeball. In this paper, we extend the polar cross-correlation technique by developing the formulas required to determine the correct location and shape of the sampling window at all eye positions. These formulas also allow the representation of three-dimensional eye position in Fick-angles, which are commonly used in oculomotor research. A numerical simulation shows the size of the errors in ocular torsion if the spherical geometry of the eye is not considered. Other effects which can affect the accuracy of video-based eye position measurements are also discussed.**

## I. Introduction

FOR A FULL understanding of the oculomotor system, as well as the afferent inputs which contribute to its control, it is necessary to measure horizontal, vertical, and torsional eye position. While dual search coils have proven to be a powerful tool for this purpose [1], [2], the expense and the invasive use of a contact lens has promoted the development of systems which determine three-dimensional (3-D) eye position from video images.

Many of the existing image processing systems for eye position measurement use some variation of the *polar cross-correlation* method [3]–[8]. Polar cross-correlation accurately measures ocular torsion in the absence of horizontal and vertical deviations of the eye, but becomes inaccurate as the eye moves to eccentric positions if the spherical geometry of the eye is not considered. An alternative technique, which takes the geometry of the eye into account and requires two distinct markers on the eye to calculate 3-D eye position, has been proposed by Nakayama [9]. This method has been realized using a contact lens to provide the markers [10] but is invasive in a manner similar to scleral search coils.

In this paper, we extend the polar cross-correlation method by developing algorithms to compensate for the geometric distortion in the projection of the eye onto the *image plane* of the camera. These geometric compensation algorithms enable accurate video-based 3-D eye position measurement over the natural range of eye movements. We also present a simulation of the errors in the measurement of ocular torsion which are induced if the geometric distortion of the image of the eye is not taken into consideration. Extensions of these simulations are used to estimate the magnitude of other effects (such as the optical effects of the cornea) on the accuracy of eye position measurements.

Manuscript received July 5, 1994; revised May 16, 1995. The work of T. Haslwanter was supported by NHMRC of Australia, Grant 920205. The work of S. T. Moore, who is the holder of an NHMRC Biomedical Postgraduate Scholarship, was supported by the Australian Brain Foundation.

T. Haslwanter is with the Department of Psychology, University of Sydney, NSW 2006 Australia.

S. T. Moore is with the Eye and Ear Research Unit, Department of Neuro-Otology, Royal Prince Alfred Hospital, Camperdown, NSW 2050 Australia.

IEEE Log Number 9414803.

## II. Methods

### A. The Polar Cross-Correlation Method

The polar cross-correlation method relies on the fact that most of the variation in pixel intensity of a digitized image of the iris occurs in the angular direction in a polar coordinate system centered on the pupil [3]. Measurement of ocular torsion can therefore be reduced to a one-dimensional signal processing task. An *iral signature* is formed by sampling pixel intensity along a circular *sampling window* on the iris at a fixed radius from the pupil center. In practice, the sampling window is often limited to a segment of this circle, as upper eyelid droop and tear build-up in the lower eye render these areas unsuitable for obtaining an iral signature. In this paper, we will employ this modified version of the polar cross-correlation method utilizing an arc-shaped sampling window.

The horizontal and vertical positions of the eye are calculated from the location of the center of the pupil in the image plane, which can be found by a number of methods, such as averaging the coordinates of the edge points of the pupil [3]. The sampling window for the determination of ocular torsion is one pixel wide and is maintained at approximately the same angular position on the iris by tracking horizontal and vertical eye movements and translating the sampling window by the same amount as the pupil center. Iral signatures from each video frame are cross-correlated with an *iral reference signature* obtained at the start of each recording. The shift in the peak of the cross-correlation function indicates the torsional position of the eye for each video frame relative to the reference image. This has been demonstrated by simultaneous measurement of ocular torsion with a video system based on polar cross-correlation and scleral search coils, which are the accepted standard for measuring 3-D eye movements [8]. So far, video-based systems have made the assumption that the geometric distortion of the shape of the sampling window at eccentric eye positions is negligible over the range of horizontal and vertical eye positions to be measured.

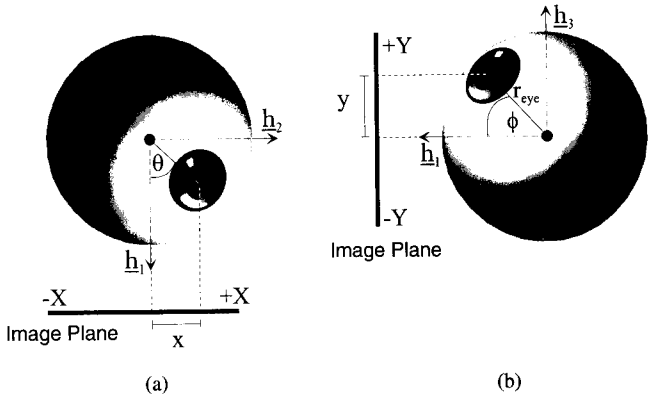


Fig. 1. (a) Top view and (b) side view of the projection of the eye onto the image plane. $\{h_1, h_2, h_3\}$ are the basis of a head-fixed coordinate system. $(x, y)$ are the coordinates of the projection of a point on the surface of the eye (in this figure the center of the pupil) onto the image plane.

The results presented below show that this assumption is invalid.

### B. Projection onto the Image Plane

The exact shape and form of the projection of the eye onto the image plane of the camera are influenced by many factors. To determine analytical formulas for the correct 3-D position of the eye from video images, we will initially make the following simplifying assumptions:

1) The eye is assumed to be a perfect sphere and rotates around the center of this sphere.
2) The eye exhibits ideal *ball and socket* behavior so that all eye movements are pure rotations around the center of the eye, with no translation of this center.
3) The camera is directly in front of the eye and the image of the eye corresponds to an orthographic projection of the eye onto the image plane, without any distortion by the optical properties of the cornea.
4) The optical axis of the eye (given approximately by the axis through the center of the pupil and the center of rotation of the eye) coincides with the visual axis, i.e., the line of sight.

To derive the mathematical formulas for the projection of the eye onto the image plane, we define a head-fixed, right-handed coordinate system $\{h_1, h_2, h_3\}$ for an upright subject, such that $h_1$ is perpendicular to the image plane and passes through the center of the pupil, $h_2$ is parallel to the interaural axis, and $h_3$ is parallel to the earth vertical axis. The center of this head-fixed coordinate system coincides with the center of the eye, and $\{h_1, h_2, h_3\}$ point forward, left, and up, respectively, as indicated in Fig. 1. The camera is oriented in such a way that the image plane is parallel to the $h_2 - h_3$ plane of the head-fixed coordinate system, and the Cartesian coordinate axes in the image plane, $x$ and $y$, are parallel to $h_2$ and $h_3$, respectively.

The projection of the center of the eye onto the image plane forms the origin of the image coordinate system. To uniquely characterize the 3-D position of the eye, we introduce an eye-fixed coordinate system $\{e_1, e_2, e_3\}$, which rotates with the eye and is oriented such that $e_1$ passes through the center of the pupil. When the eye is in the reference position, i.e., looking straight ahead, $\{e_1, e_2, e_3\}$ are chosen such that they coincide with $\{h_1, h_2, h_3\}$. A head-fixed *reference point* $p_{\text{ref}}$ is given by the intersection of the surface of the eye with $h_1$

$$p_{\text{ref}} = r_{\text{eye}} * (1, 0, 0) \tag{1}$$

where $r_{\text{eye}}$ is the radius of the eyeball. Every point $p$ on the surface of the eye can then be described by a rotation matrix $\mathbf{R}$ which characterizes the rotation from the reference point $p_{\text{ref}}$ to the current point $p$

$$p = \mathbf{R} \cdot p_{\text{ref}} = r_{\text{eye}} * (R_{11}, R_{21}, R_{31}) \tag{2}$$

where $R_{ij}$ is the matrix element in the $i$th row and $j$th column of the rotation matrix $\mathbf{R}$.

Let $\mathbf{R}$ be composed of a horizontal rotation about $e_3$ by $\theta$, followed by a vertical rotation about the *rotated* axis $e_2$ by $\phi$. Such descriptions of rotations, in which consecutive rotations are executed about eye-fixed axes, are often called *passive rotations* or *rotations of the coordinate system.* The rotation matrix $\mathbf{R}(e_3, \theta)$, which describes the rotation of an object about the axis $e_3$ by $\theta$, is given by

$$\mathbf{R}(e_3, \theta) = \begin{bmatrix} \cos(\theta) & -\sin(\theta) & 0 \\ \sin(\theta) & \cos(\theta) & 0 \\ 0 & 0 & 1 \end{bmatrix} \tag{3}$$

and the rotation about the axis $e_2$ by $\phi$ is described by

$$\mathbf{R}(e_2, \phi) = \begin{bmatrix} \cos(\phi) & 0 & \sin(\phi) \\ 0 & 1 & 0 \\ -\sin(\phi) & 0 & \cos(\phi) \end{bmatrix}. \tag{4}$$

Equations (1) and (2) show how these rotation matrices can be used to characterize rotations of a point on the surface of the eye, such as the center of the pupil. Interpreting the columns of the unit matrix $\mathbf{I}_3$ as three unit vectors aligned with $\{h_1, h_2, h_3\}$ respectively, the columns of a rotation matrix $\mathbf{R}$ can be interpreted as the components of these vectors in the head-fixed coordinate system after they have undergone a rotation described by $\mathbf{R}$. For example, a rotation about the vertical axis, characterized by $\mathbf{R}(e_3, \theta)$, rotates the $h_2$-aligned vector (0, 1, 0) into the vector $(-\sin(\theta), \cos(\theta), 0)$. Detailed explanations of the vector- and matrix-formalism can be found in most linear algebra texts, and a more extensive description of the application of rotation matrices to eye movements is given in [11].

The combined matrix $\mathbf{R}(\theta, \phi)$, which describes the rotation from the reference point $p_{\text{ref}}$ to the current point $p$, is given by

$$\begin{aligned} \mathbf{R}(\theta, \phi) &= \mathbf{R}(e_3, \theta) \cdot \mathbf{R}(e_2', \phi) \\ &= \begin{bmatrix} \cos(\theta)\cos(\phi) & -\sin(\theta) & \cos(\theta)\sin(\phi) \\ \sin(\theta)\cos(\phi) & \cos(\theta) & \sin(\theta)\sin(\phi) \\ -\sin(\phi) & 0 & \cos(\phi) \end{bmatrix} \end{aligned} \tag{5}$$

The prime in $e_2'$ indicates that the rotation is about the *rotated* eye-fixed axis $e_2$. Since rotations are noncommutative, the

sequence of the rotation matrices $\mathbf{R}(e_3, \theta)$ and $\mathbf{R}(e_2, \phi)$ is important and can not simply be reversed. The projection of the point $p$ onto the image plane, $(x, y)$, is graphically represented in Fig. 1. It is given by the second and third vector component in (2).

$$\begin{pmatrix} x \\ y \end{pmatrix} = r_{\text{eye}} * \begin{pmatrix} R_{21} \\ R_{31} \end{pmatrix}. \tag{6}$$

Substitution of (5) and (6) gives

$$\begin{pmatrix} x \\ y \end{pmatrix} = r_{\text{eye}} * \begin{pmatrix} \sin(\theta)\cos(\phi) \\ -\sin(\phi) \end{pmatrix}. \tag{7}$$

### C. Determination of Three-Dimensional Eye Position

Since the matrix $\mathbf{R}(\theta, \phi)$ can be used to describe any point on the surface of the eye, it can also be used to characterize the center of the pupil, and thus the line of sight. This matrix does not specify the 3-D position of the eye completely however, as the rotation about the line of sight is still undefined. To uniquely characterize the rotation of the eyeball from the reference position to the current position, we can use a sequence of a horizontal rotation about $e_3$ by $\theta$, followed by a vertical rotation about the rotated axis $e_2$ by $\phi$, and a torsional rotation about the twice rotated line of sight $e_1$ by $\psi$. This sequence of rotations is often used in oculomotor research, and is called the *Fick sequence* [12]. It corresponds to the rotation matrix

$$\mathbf{R}_{\text{Fick}} = \mathbf{R}(e_3, \theta) \cdot \mathbf{R}(e_2', \phi) \cdot \mathbf{R}(e_1'', \psi) \tag{8}$$

with $e_1''$ indicating the twice rotated axis $e_1$, and $\mathbf{R}(e_1, \psi)$ defined as

$$\mathbf{R}(e_1, \psi) = \begin{bmatrix} 1 & 0 & 0 \\ 0 & \cos(\psi) & -\sin(\psi) \\ 0 & \sin(\psi) & \cos(\psi) \end{bmatrix}. \tag{9}$$

In the following, we will refer to $\psi$ as *Fick torsion*, since this value depends not only on the position of the eye, but also on this particular sequence of rotations.

The polar cross-correlation method uses the pupil center coordinates in the image plane $(x_p, y_p)$ to obtain estimates of the horizontal and vertical eye position $(\theta_p, \phi_p)$ by inverting (7). The shift in the peak of the cross-correlation of an iral signature with the iral reference signature gives the torsional component $\psi$ of the eye position. However, this approach is only valid in the absence of horizontal or vertical eye movements. When the eye is in an eccentric position, the projection of the sampling window onto the image plane will deviate from the original shape. Simply translating the original sampling window in the image plane by the same amount as the pupil center does not take this geometric distortion into account, and an iral signature would be obtained from the wrong area of the iris. When this incorrect iral signature is cross-correlated with the iral reference signature, an erroneous value for ocular torsion is indicated. In the following, we call these purely translated arcs geometrically *uncompensated* sampling windows. The next section will discuss how the correct (geometrically *compensated*) position of the sampling window can be determined for any horizontal and vertical eye position.

## III. Results

### A. Compensation for Geometric Distortion

When the eye is in the reference position, as in Fig. 2(a), the center of the pupil coincides with the reference point $p_{\text{ref}}$. An arc-shaped sampling window is formed in the image plane, and for each point $(x_a, y_a)$ on this arc the corresponding projection onto the surface of the eye $(\theta_a, \phi_a)$ can be determined by inverting (7). The position of every point on a sampling window is then uniquely determined by $\mathbf{R}_{\text{arc}} = \mathbf{R}(\theta_a, \phi_a)$, given by (5). When the eye has moved to an eccentric position, the coordinates of the center of the pupil in the image plane $(x_p, y_p)$ can be determined by averaging the coordinates of the pupil edge points. Inverting (7) we can calculate the Fick angles of the pupil center $(\theta_p, \phi_p)$, which uniquely determine $\mathbf{R}_{\text{pupil}} = \mathbf{R}(\theta_p, \phi_p)$. Note that $\mathbf{R}_{\text{pupil}}$ not only brings the center of the pupil from the reference position to the current position, but also places the eye in a position with zero Fick torsion. Combining the two rotations—the first of which brings the eyeball from the reference position to the current position with zero Fick torsion, and the second of which describes the rotation from the center of the pupil to a point on the sampling window—we can, for each point of the sampling window, determine the matrix $\mathbf{R}_{\text{total}}$ which describes the combined rotation from the reference point to the current position of the sampling point on the eyeball

$$\mathbf{R}_{\text{total}} = \mathbf{R}_{\text{pupil}} \cdot \mathbf{R}_{\text{arc}}. \tag{10}$$

From $\mathbf{R}_{\text{total}}$ and (6) we can determine the location of the points of the geometrically compensated sampling window in the image plane $(x_c, y_c)$ for the current eye position $(\theta_p, \phi_p)$ as shown in (11) at the bottom of the following page.

Cross-correlation of the iral signature obtained from the compensated sampling window with the iral reference signature gives the Fick torsion of the eye. Fig. 2 illustrates the effect of the geometric compensation. Fig. 2(a) shows a sketch of the eye in the reference position. The four arcs indicate the location of four different sampling windows with a span of 60°, centered on the $x$- and $y$-axes. Fig. 2(b) shows the same

$$\begin{aligned} \begin{pmatrix} x_c \\ y_c \end{pmatrix} &= r_{\text{eye}} * \begin{pmatrix} (R_{\text{total}})_{21} \\ (R_{\text{total}})_{31} \end{pmatrix} \\ &= r_{\text{eye}} * \begin{pmatrix} \sin(\theta_p)\cos(\phi_p)\cos(\theta_a)\cos(\phi_a) + \cos(\theta_p)\sin(\theta_a)\cos(\phi_a) - \sin(\theta_p)\sin(\phi_p)\sin(\phi_a) \\ -\sin(\phi_p)\cos(\theta_a)\cos(\phi_a) - \cos(\phi_p)\sin(\phi_a) \end{pmatrix}. \end{aligned} \tag{11}$$

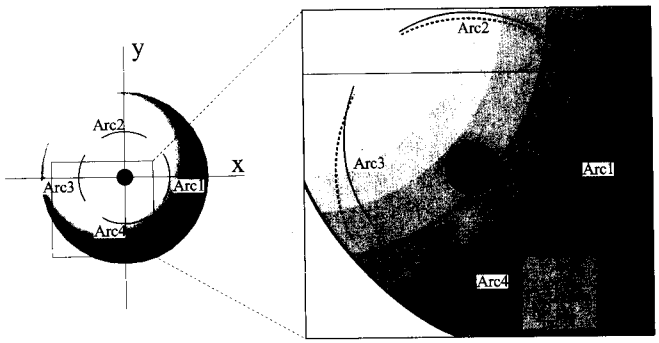


Fig. 2. Diagram of the projection of the eye onto the image plane. (a) Eye in the reference position, with four arc-shaped sampling windows indicated by the solid black lines. (b) Line of sight directed 20° right and 20° down. Dashed lines indicate the translated sampling windows; solid lines show location and shape of the properly compensated arcs. $\Delta_x$ and $\Delta_y$ indicate the horizontal and vertical shift in the image plane from a compensated point $P_c$ to the corresponding uncompensated point $P_{\rm uc}$.

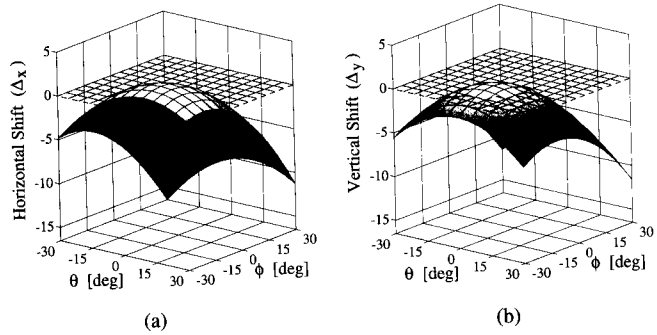


Fig. 3. (a) Horizontal shift ($\Delta_x$) and (b) vertical shift ($\Delta_y$) from compensated points to uncompensated points in the image plane, when the line of sight is directed 20° right and 20° down [see also Fig. 2(b)]. The Fick angles $\theta$ and $\phi$ indicate the horizontal and vertical position of these points on the eyeball when the eye is in the reference position. The shift is expressed as a percentage of the radius of the eyeball.

eye, with the eye rotated 20° to the right (from the subject's point of view), and 20° down.

The solid and dashed lines show the compensated and uncompensated (i.e., purely translated) sampling windows, respectively. One can see that the compensated sampling windows have undergone a nonlinear translation and deformation from their original shape. This deformation depends on the eye position, as well as on the original location and size of the sampling window. The horizontal shift ($\Delta_x$) and vertical shift ($\Delta_y$) between the geometrically compensated projection of a point $P_c$ on $Arc4$ and the corresponding purely translated (uncompensated) point $P_{\rm uc}$ are indicated.

Fig. 3 shows the magnitude of $\Delta_x$ and $\Delta_y$ for points on the eyeball within a 30° range from the center of the pupil, with the eye rotated 20° to the right and 20° down, as shown in Fig. 2(b). The Fick angles $\theta$ and $\phi$ indicate the horizontal and vertical position of these points on the eyeball when the eye is in the reference position (Fig. 2(a)). Note that while the center of the pupil ($\theta = \phi = 0°$) is in the correct location, all other points are shifted horizontally and/or vertically. The magnitudes of these shifts depend on the orientation of the eye, and are different for each eye position.

### *B. Simulation of Geometric Distortion*

To determine the errors in ocular torsion that would be caused by using the four uncompensated sampling windows in Fig. 2, we have developed a simulation of torsion measurement using polar cross-correlation, and applied it to a range of horizontal and vertical eye positions with zero Fick torsion. To simulate the iral pattern, we have performed a frequency analysis on an iral signature recorded with a video system in our laboratory (VTM [6]) from a human subject, and generated an iral test-pattern using the dominant frequency components (Fig. 4(a), solid line). For simplification, we have made the assumption that the iris has a purely radial pattern [3]. Typical values from the VTM system have been used for the radius of the eye (300 pixels) and the radial distance of the sampling windows from the center of the pupil (160 pixels). The simulation was written in MATLAB (The MathWorks, Inc.) and works as follows.

With the eye in the reference position, we place four arc-shaped sampling windows on the image plane, as indicated in Fig. 2(a) (span of 60°, centered on the $x$ and $y$ axes). We then determine the location of the center of the pupil in the image plane for a given horizontal and vertical orientation of the eye with (7). The sampling windows are then translated by the same amount as the pupil center (Fig. 2(b), dashed lines). To determine the iral signatures along these uncompensated arcs, we change the parametrization of $\mathbf{R}_{\rm arc}$ from that of (5) to

$$\mathbf{R}_{\rm arc} = \mathbf{R}(e_1, \alpha) \cdot \mathbf{R}(e_3', \beta) = \begin{bmatrix} \cos(\beta) & -\sin(\beta) & 0 \\ \cos(\alpha)\sin(\beta) & \cos(\alpha)\cos(\beta) & -\sin(\alpha) \\ \sin(\alpha)\sin(\beta) & \sin(\alpha)\cos(\beta) & \cos(\alpha) \end{bmatrix} \tag{12}$$

which describes the rotation from the center of the pupil to a point on the iris by a rotation about the line of sight $e_1$ by $\alpha$, followed by a rotation about the (rotated) axis $e_3$ by $\beta$.

If we describe a point $p$ on the iris by $\mathbf{R}(\alpha, \beta)$, the simulated iral intensity at $p$ is only determined by the radial component $\alpha$, which can be calculated from (12) as

$$\alpha = \arctan\left(\frac{(R_{\rm arc})_{31}}{(R_{\rm arc})_{21}}\right). \tag{13}$$

For each point on the sampling window, $\mathbf{R}_{\rm arc}$ can be obtained by transforming (10) to

$$\mathbf{R}_{\rm arc} = \mathbf{R}_{\rm pupil}^{-1} \cdot \mathbf{R}_{\rm total}. \tag{14}$$

Using (5) and (7), $\mathbf{R}_{\rm pupil} = \mathbf{R}(\theta_p, \phi_p)$ can be obtained from $(x_p, y_p)$ as described in the previous section. Note that $\mathbf{R}_{\rm pupil}$ consists only of a rotation about the vertical axis, followed by a rotation about the horizontal axis, and thus places the simulated eye in a position with zero Fick torsion. $\mathbf{R}_{\rm total} = \mathbf{R}(\theta_t, \phi_t)$ can be determined in the same way from the position of the translated sampling window. From (13) and (14), and the fact that rotation matrices are orthogonal with $\mathbf{R}^T = \mathbf{R}^{-1}$, $\alpha$ can then be obtained explicitly as (15), shown at the bottom of the following page.

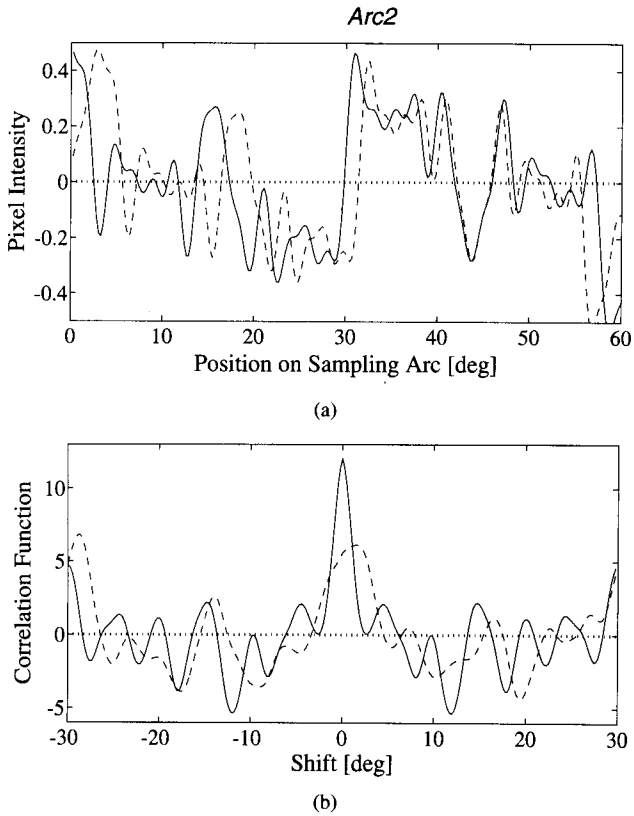


Fig. 4. (a) Compensated iral signature (solid line), which is equivalent to the iral reference signature, and uncompensated iral signature (dashed line). The iral signatures were taken from $Arc2$ in Fig. 2(b), with the eye 20° right and 20° down from the reference position. (b) Cross-correlation function of the compensated iral signature with the iral reference signature (solid line), and of the uncompensated iral signature with the iral reference signature (dashed line).

Fig. 4(a) shows the compensated and uncompensated iral signatures for $Arc2$, with the eye looking 20° right and 20° down, as shown in Fig. 2(b). The solid line is the iral signature taken along the compensated arc and is equivalent to the iral reference signature, since the eye has zero Fick torsion; the dashed line shows the iral signature along the uncompensated sampling window and has been determined using (15). One can clearly see the deformation of the pattern: while the two patterns superpose at approximately 45°, features at either end of this iral signature are shifted in opposite directions. This is due to the error in positioning of the uncompensated sampling window, as demonstrated by Figs. 2 and 3. Cross-correlation of such a signature with the iral reference signature leads to incorrect values for ocular torsion. Fig. 4(b) shows the results of the cross-correlation of the two patterns with the iral reference signature: while the cross-correlation of the compensated iral signature with the iral reference signature (solid line) is equivalent to the auto-correlation of the iral reference signature and correctly shows zero Fick torsion, the peak of the cross-correlation of the uncompensated iral signature with the iral reference signature (dashed line) is shifted by approximately 1.5°, and thus incorrectly indicates ocular torsion. Note that the latter cross-correlation function is so distorted that the global maximum of the uncompensated cross-correlation trace is not in the vicinity of zero, but at approximately −28°. To avoid such extreme errors at large horizontal and vertical angles, we have restricted the search for the peak of the cross-correlation function in our simulation to a range of ±10°, which corresponds to the naturally occurring range of ocular torsion in humans.

We have performed the procedures outlined above for eye positions from −20° to +20°, horizontally and vertically, in 2.5° steps. The erroneous torsion indicated by the polar cross-correlation using the uncompensated sampling windows is shown in Fig. 5.

The torsion indicated is different for each arc and depends strongly on the eye position. There is a close symmetry between the results for the two horizontal arcs $Arc1$ and $Arc3$, and the two vertical arcs $Arc2$ and $Arc4$. The different shape of the surfaces for the horizontal and vertical arcs is due to the asymmetry between horizontal and vertical movements in the Fick sequence of rotations: horizontal movements are always about the axis $h_3$, whereas the vertical movements are about the rotated axis $e_2$. Changing parameters in the simulation revealed that the torsional values obtained by taking the iral signature along the uncompensated arcs also show a small dependency on the frequency components of the iral signature, as well as on the radius of the sampling window. However, these dependencies are eliminated by using the compensated sampling windows to obtain the iral signatures. We have also run the simulation using the compensated sampling windows, and zero Fick torsion is correctly indicated over the entire range of horizontal and vertical eye positions.

### C. Simulation of Other Effects

The derivation of the formulas in the preceding sections relies on a number of assumptions. We have extended our simulation, using the same parameters as above, to investigate the validity of these assumptions and their effect on measured eye position values. Note that in all the simulations below, the iral signatures are calculated using geometrically compensated sampling windows.

*1) Translations of the Eyeball:* One problem is that the eye does not exhibit ideal "ball and socket" behavior. During vergence, lateral translations of the eye in the orbit of up to 200 μm occur [13], which would appear to a video-based system to be a horizontal rotation of around 1°. Including such a shift in our simulation shows that misinterpreting such a translation as a rotation can induce an error in the measurement of ocular torsion of up to 0.23°.

*2) Errors in Finding the Center of the Pupil:* If the location of the center of the pupil is not determined correctly, the

$$\alpha = \arctan\left(\frac{\cos(\theta_t)\cos(\phi_t)\cos(\theta_p)\sin(\phi_p) + \sin(\theta_t)\cos(\phi_t)\sin(\theta_p)\sin(\phi_p) - \sin(\phi_t)\cos(\phi_p)}{-\cos(\theta_t)\cos(\phi_t)\sin(\theta_p) + \sin(\theta_t)\cos(\phi_t)\cos(\theta_p)}\right). \quad (15)$$

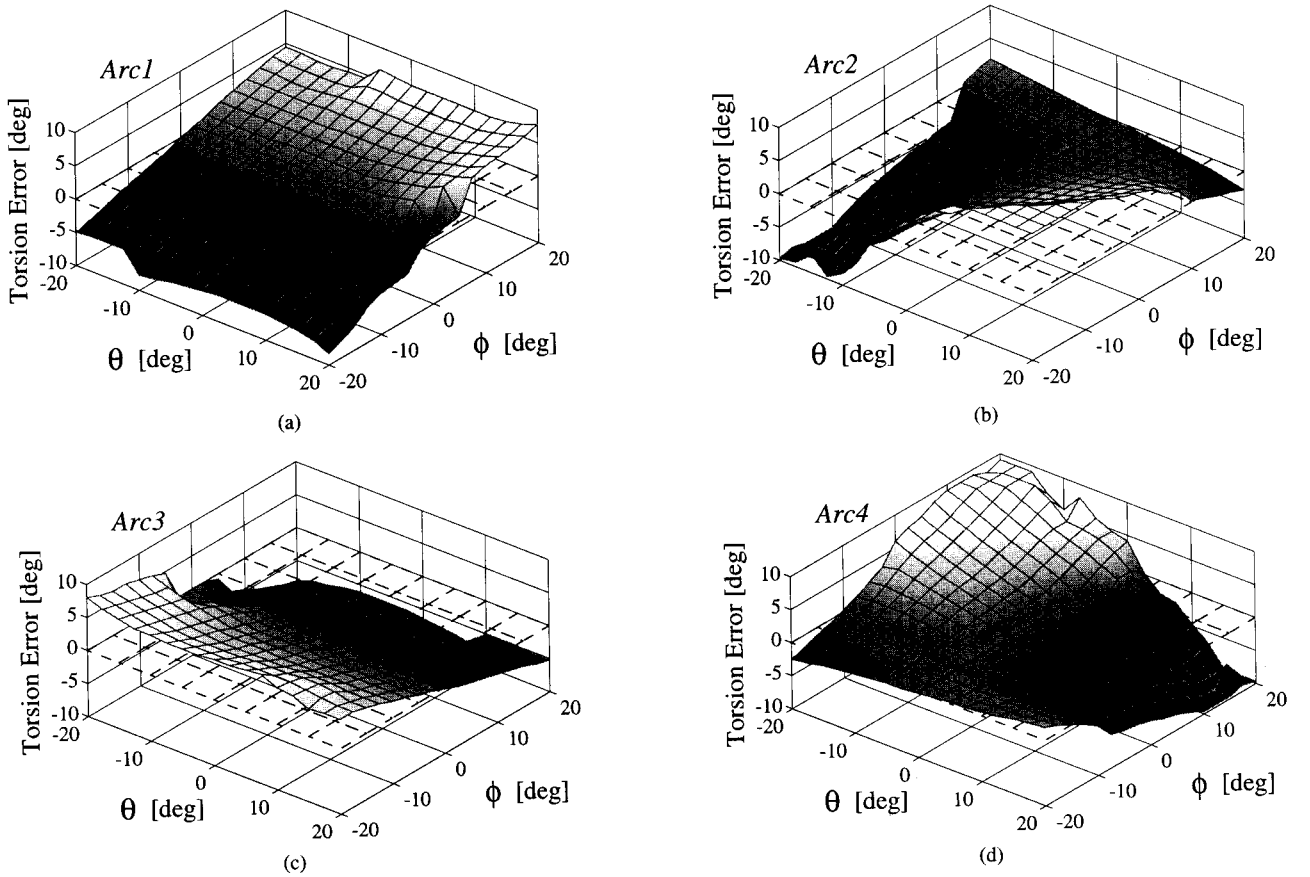


Fig. 5. Numerical simulation of the Fick torsion indicated by the four uncompensated arcs in Fig. 2. In the simulation, the eye has been placed in horizontal and vertical positions with zero Fick torsion, so any torsional value different from zero constitutes an error. The dashed grids indicate zero torsion. (a) Arc 1, (b) Arc 2, (c) Arc 3, (d) Arc 4.

sampling arcs will also be placed in the wrong position. We have first put the eyeball in different horizontal and vertical positions with zero Fick torsion, then introduced a shift in the location of the center of the pupil, and finally calculated the location of the compensated sampling windows using that shifted pupil-center. If the center of the pupil was shifted by 0.2 mm, which corresponds to an eye movement of about 1°, the simulation indicated an erroneous ocular torsion of up to 1.9°, depending on the direction of the shift and the location of the sampling window.

*3) Effects of the Cornea on Finding the Center of the Pupil:* Assuming that the iris is a flat disk located 3 mm behind the apex of the cornea [14], we have determined the apparent shift in the location of the center of the pupil caused by the optical properties of the cornea as follows. Using Gullstrand's model of the eye, we replaced the cornea by a single thin lens with a focal length of 31.6 mm, positioned 0.5 mm in front of the corneal vertex [15], [16]. A change in the distance between this lens and the pupil will lead to a change in the magnification of the image of the pupil. Assuming that the cornea is a perfect sphere with a radius of 8 mm, we determined the horizontal distance between the upper edge of the pupil and the cornea when the subject looks straight ahead [$P_0P_2$ in Fig. 6(a)], 20° down ($P_0P_1$), and 20° up ($P_0P_3$). Using the thin lens equation from paraxial optics, we then determined the change of the magnification of the image of the upper and lower edge of the pupil due to the change in this distance at different eye positions. The different magnification factors for the upper and the lower edge of the pupil cause a shift in the apparent location of the pupil center. We have run this model with pupil radii of 1.2 and 4 mm, and the resulting maximum error for the determination of the pupil center for eye movements within ±20° was 0.04° and 0.35°, respectively. A pupil radius of 1.2 mm is typical for measurements with the VTM system [6], where the pupil is deliberately constricted by the use of pilocarpine hydrochloride; a radius of 4 mm corresponds to a large pupil in a young adult. Note that these calculations give only an approximate estimate of the effect, especially for the larger pupil diameter, since the surface of the cornea is in fact not a perfect sphere.

*4) Effects of the Cornea on the Iral Signature:* The optical properties of the cornea lead not only to a distortion of the image of the pupil, but also of the image of the iris itself. In a manner analogous to that described above, we have calculated the shift of the image of the upper and lower extremities of a circular sampling window when the eye looks 20° up, labeled $\Delta_{\text{top}}$ and $\Delta_{\text{bottom}}$ respectively in Fig. 6(b). We have taken the horizontal distance between the cornea and the iris at this point to be 1.8 mm, the radius of the cornea 10 mm (to allow for flattening of the cornea at the outer extremities [14]), and the center of this corneal sphere to be located on